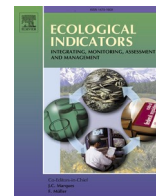


Contents lists available at [ScienceDirect](https://www.sciencedirect.com)

Ecological Indicators

journal homepage: www.elsevier.com/locate/ecolind

A new early warning indicator of tree species crashes from effective intraspecific interactions in tropical forests

Hugo Fort^{a,*}, Tomás S. Grigera^{b,c}^a *Institute of Physics, Faculty of Science, Universidad de la República, Iguá 4225, Montevideo 11400, Uruguay*^b *Instituto de Física de Líquidos y Sistemas Biológicos, CONICET & Universidad Nacional de La Plata, La Plata, Argentina*^c *CCT CONICET La Plata, Consejo Nacional de Investigaciones Científicas y Técnicas, Argentina, Departamento de Física, Facultad de Ciencias Exactas, Universidad Nacional de La Plata, Argentina*

ARTICLE INFO

Keywords:

Early warning indicators, Species loss
Ecosystem collapse
Tropical forest dynamics
Maximum entropy method

ABSTRACT

The vulnerability of species richness to several factors like, climate change, habitat fragmentation, resource exploitation, etc., poses a challenge to conservation biologists and agencies working to sustain the ecosystem services. Hence, there is a clear need for early warning indicators of species loss generated from empirical data.

The tree community of the long-term 50-hectare plot on Barro Colorado Island (BCI), Panama, is one of the most intensively studied in the world. This plot was established in 1981 and fully censused in 1982 then every 5 years from 1985 through 2015. This extensive dataset reveals that some tree species suffered steep population declines.

Here we propose an early warning indicator of such tree population crashes and test it against the BCI dataset. The spatial covariance matrices, C_{ij} , of the 20 most abundant tree species in BCI allow us to compute, via MaxEnt, the effective interaction matrices, J_{ij} , among these species for the eight censuses available from 1982 to 2015. For each species i and each census c , the absolute value of the intraspecific competition coefficients $J_{ii}(c)$ are much larger than those of the interspecific interaction coefficients $J_{ij}(c)$ with $i \neq j$. We show that this result can be derived from a similar empirical relationship observed for the matrices $C_{ii}(c)$. Our main finding is that for those tree species that suffered steep population declines (of at least 50%), across the eight tree censuses, the drop of J_{ii} is always steeper and occurs before the drop of the corresponding species abundance N_i . Indeed, such sharp declines in J_{ii} occur between 5 and 15 years in advance than comparable declines for N_i , and thus they serve as early warnings of impending population busts. Furthermore, this drop of J_{ii} is linked to the anomalous variance, which is a known early warning of incoming catastrophic shifts.

1. Introduction

The rate of species loss we are observing around the world is much greater than anything experienced historically (Thompson and Starzomski, 2006). Diversity loss, combined with environmental change, increases the risk of abrupt and potentially irreversible ecosystem collapse (Ives and Carpenter, 2007; Hooper et al., 2012; MacDougall et al., 2013). Such catastrophic ecological regime shifts may be announced in advance by early warning signals such as slowing return rates from perturbation and rising variance (Carpenter et al., 2011). Thus, it is difficult to overstate the importance of identifying early warning signals that would allow managers to predict catastrophic biodiversity losses before they happen so that they can take remedial

action.

The issue of fluctuations of biodiversity is closely related with a major debate in ecology of whether species coexistence emerges from equilibrium niche partitioning or from non-equilibrium stochastic dispersal-assembly (Clark and McLachlan, 2003; Ishida et al., 2003). According to the first hypothesis, in a community at equilibrium each species occupies a different niche that results from and reduces direct competition (Whittaker, 1975). Stabilizing mechanisms – like tradeoffs between species in terms of their capacities to disperse to sites where competition is weak, to exploit abundant resources effectively and to compete for scarce resources (Clark and McLachlan, 2003) – play an important role. Alternatively, the dispersal-assembly hypothesis assumes that communities are open nonequilibrium assemblages of

* Corresponding author.

E-mail address: hugo@fisica.edu.uy (H. Fort).

<https://doi.org/10.1016/j.ecolind.2021.107506>

Received 12 August 2020; Received in revised form 5 February 2021; Accepted 6 February 2021

Available online 22 February 2021

1470-160X/© 2021 The Author(s).

Published by Elsevier Ltd.

This is an open access article under the CC BY-NC-ND license

(<http://creativecommons.org/licenses/by-nc-nd/4.0/>).

species that coexist only transiently through by chance, history, and random dispersal rather than by the stabilizing effects of niche differentiation, regarded as superfluous (Hubbell, 2008, 2009). This ‘neutral model’ thus emphasizes ‘equalizing’ mechanisms (Chesson, 2000), because competitive exclusion of similar species is slow. The relative importance of these two mechanisms is still a matter of discussion. It was argued that stabilizing processes and fitness inequality vary among communities and respond to anthropogenic changes (Adler et al., 2007). However, strong evidence was found that patterns of habitat association (and hence conclusions on the importance of niche vs neutral processes) are affected by the choice of sampling scale (Garzon-Lopez et al., 2014; Chase, 2014). Indeed, Garzon-Lopez et al. (2014) found that the very BCI tropical forest is highly niche-structured at large scales, and largely neutrally structured at small scales.

The tree community of the long-term 50-hectare plot on Barro Colorado Island (BCI), Panama, is one of the most intensively studied in the world. This plot was established in 1981 and fully censused in 1982 then every 5 years from 1985 through 2015. All stems ≥ 1 cm diameter-at breast-height (dbh) were mapped, measured, and identified in each census (Condit et al., 2017). These data from eight censuses of trees spanning 35 years is a period long enough to examine decadal changes in tree growth rates and death rates. They demonstrate that the BCI forest has exhibited considerable dynamism in this period. A variety of population trajectories can be observed: busts, recoveries and oscillations (Condit et al., 2017).

For this tree community of the 50-hectare BCI plot, using the maximum entropy (MaxEnt) principle, Volkov et al., 2009 estimated the ‘effective’ interaction strengths between species for the 20 most abundant species for trees (dbh ≥ 1 cm) in the 50-hectare BCI plot at the first census (1982). Their estimates for interspecific interaction coefficients are generally an order of magnitude smaller than those for intraspecific coefficients (Volkov et al., 2009). Using the same MaxEnt procedure we recently verified that for the next seven available censuses (1985 and then every five years until 2015) the interspecific effective interaction coefficients are also generally much smaller than the intraspecific ones (Fort and Grigera, 2020). Indeed, this finding is in agreement with empirical evidences supporting that pairwise interspecific interaction strengths are often much weaker than the intraspecific ones from plants (Adler et al., 2018) and across several taxonomic groups (Fort and Segura, 2018). Larger intraspecific competition relative to interspecific competition is also a result expected from theoretical grounds, to ensure the stable coexistence of multispecies communities (Chesson, 2000).

Here, we are interested in providing early warnings before crashes of species occur. There is increasing evidence that ecosystems can pass thresholds and go through catastrophic regime shifts (Scheffer and Carpenter, 2003) where sudden and large changes in their functions take place. Most importantly, these changes are very difficult and costly to reverse. Thus, an important problem in environmental sciences is to get early warning signals of these impending catastrophic regime shifts in ecosystems to allow addressing currently intractable problems in ecosystem management, such as the avoidance of ecological surprises, and the maintenance of systems in desired states (Fort, 2020). The issue of providing early warning signals of catastrophic events in ecosystems has been addressed by different methods (Dakos et al., 2010, Donangelo et al., 2010, Suweis and D’Odorico, 2014, Doncaster et al., 2016, Saravia and Momo, 2018).

In addition to the above mentioned finding, that intraspecific

ⁱ We stress the effective character of these interaction coefficients since they result from the multiple biotic interactions among the species as well as from the abiotic interaction between species and the environment. Mathematically this arises because, as we show in the Methods section, this interaction matrix is minus the inverse of the covariance matrix, and therefore its elements include products over all the S species making up the community (rather than just pairs as in the case of the covariance matrix).

interactions between trees in BCI are much larger than the interspecific interactions (Fort and Grigera, 2020), we also showed that self-regulation by intraspecific competition seems to control the trajectories (i.e. the corresponding sequences of abundances over censuses) of several species in the BCI plot (Fort and Grigera, 2020). This opens the possibility that the intraspecific interaction coefficients could provide early warnings for impending species crashes. Hence, firstly we derived analytically this result about the dominance of the intraspecific interaction coefficients from a corresponding difference in size between covariances and variances. Secondly, we focused on these diagonal elements of the estimated interaction matrices, analyzing if their behavior serve to provide early warnings for species that crashed before they did it.

2. Methods

2.1. Using the MaxEnt principle to estimate the effective interaction matrix between species of trees

The maximum entropy (MaxEnt) principle is a general method to make the least biased inferences compatible with available data (Jaynes, 1957a, 1957b). That is, the lack of knowledge we generally have on a real system can be modeled by a probability distribution for the different possible states of that system. However, a common problem on top of this is that this probability distribution is not known, and there are many different probability distributions for the states of the system which are compatible with available data. Of all such distributions, the recipe of MaxEnt is to choose the probability distribution that maximizes the Shannon’s information entropy (Shannon, 1948) subject to the constraints of the information.ⁱⁱ

In our case, the system is the community of trees of BCI composed of S coexisting species for each of which we have spatial information on the location of every individual. With the aim to use these data to infer the effective interaction strengths between the species we follow the procedure of Volkov et al. (2009). That is, to deduce various correlations from such spatial data, we divide the 50-hectare plot into equally sized quadrats large enough to contain many individuals yet small enough to have a sufficient number of quadrats to facilitate statistical averaging. Quadrats of 20 m of side serve to solve this trade-off. Therefore we have a number of quadrats $Q = 500,000 \text{ m}^2 / 400 \text{ m}^2 = 1250$. The state of a quadrat is specified by the set of the densities for each species within this quadrat $\{x_i\}$, where x_i is the density of the i th species in this particular quadrat (a real variable). Let us arrange these densities into a row vector $\mathbf{x}^T = [x_1, x_2, \dots, x_S]$, where the superscript ‘T’ stands for ‘transpose’ which transforms an ordinary column vector into a row one \times (in such a that given two vectors \mathbf{a} and \mathbf{b} , the product $\mathbf{a}^T \mathbf{b} = \sum_i a_i b_i$ is a scalar quantity). And denote the corresponding multivariate probability distribution of S random variables by $P(\mathbf{x})$, which by definition obeys the normalization condition:

$$\int d\mathbf{x} P(\mathbf{x}) = \int \prod_i dx_i P(\mathbf{x}) = 1. \quad (1)$$

The Shannon’s information entropy, H , is thus written in terms of $P(\mathbf{x})$ as (Shannon, 1948; Jaynes, 1957a):

$$H = - \int d\mathbf{x} P(\mathbf{x}) \ln P(\mathbf{x}) = - \int \prod_i dx_i P(\mathbf{x}) \ln P(\mathbf{x}), \quad (2)$$

where \ln denotes the natural logarithm. For simplicity of notation it is convenient to denote expected values of quantities X , by $E[X]$. For

ⁱⁱ Readers unfamiliar with the maximum entropy principle can find overviews about how concepts like, Shannon entropy, constraints, probability distributions and the partition function are applied to ecology in either Volkov et al. (2009), Harte (2011) Brummer & Newman (2019) or Fort (2020),

example, equations (1) and (2) become

$$E[1] = 1, \tag{1'}$$

$$-E[\ln P(\mathbf{x})] = H. \tag{2'}$$

Here as known constraints, in addition to (1'), we consider that the first two statistical moments, the mean densities and covariances, match the corresponding sample mean values over Q measurements. These constraints on the distribution are then expressed as expected values as:

$$E[x_i] = \bar{x}_i \equiv \sum_{\mu=1}^Q x_i^\mu / Q, \tag{3a}$$

$$E[(x_i - E[x_i])(x_j - E[x_j])] = \overline{(x_i - \bar{x}_i)(x_j - \bar{x}_j)} = \bar{x}_i \bar{x}_j - \bar{x}_i \bar{x}_j = \sum_{\mu=1}^Q x_i^\mu x_j^\mu / Q - \sum_{\mu=1}^Q x_i^\mu \sum_{\nu=1}^Q x_j^\nu / Q^2, \tag{3b}$$

where a bar over a quantity denotes its sample average and the indices μ and ν denote quadrats (we use Greek indices, running from 1 to Q , to distinguish them from Latin indices denoting species, thus running from 1 to S). The idea is to obtain the effective interaction strengths between tree species from the expression of the probability distribution that maximizes the information entropy with constraints. A well known analytical technique to obtain the maximum entropy probability distribution $P(\mathbf{x})$ consistent with the constraints (1'), (3a) and (3b) is the method of the Lagrange multipliers (Arfken, 1985), which converts a constrained maximization problem into an unconstrained one by maximizing

$$H' = H - \lambda_0(E[1] - 1) - \sum_{i=1}^S h_i(E[x_i] - \bar{x}_i) - \frac{1}{2} \sum_{i,j=1}^S J_{ij}(E[x_i x_j] - \bar{x}_i \bar{x}_j), \tag{4}$$

where λ_0 is a scalar Lagrange multiplier, h_i are the elements of a vector \mathbf{h} of Lagrange multipliers and J_{ij} the elements of a matrix \mathbf{J} of Lagrange multipliers corresponding, respectively, to constraints (1), (3a) and (3b). As we will show in brief, J_{ij} can be naturally interpreted as the interaction coefficient of species j over species i . The maximizing probability distribution is obtained by setting the functional derivative H' with respect to the unknown $P(\mathbf{x})$ to zero (Jaynes, 1982):

$$0 = \frac{\delta H'}{\delta P(\mathbf{x})} = - \frac{\delta \left(E[\ln P(\mathbf{x})] + \lambda_0 E[1] - \sum_{i=1}^S h_i E[x_i] - \frac{1}{2} \sum_{i,j=1}^S J_{ij} E[x_i x_j] \right)}{\delta P(\mathbf{x})} = - \frac{\delta \left(\int d\mathbf{x} P(\mathbf{x}) \left(\ln P(\mathbf{x}) + \lambda_0 - \sum_{i=1}^S h_i x_i - \frac{1}{2} \sum_{i,j=1}^S J_{ij} x_i x_j \right) \right)}{\delta P(\mathbf{x})} \tag{5}$$

which produces $\ln P(\mathbf{x}) + 1 + \lambda_0 - \sum_{i=1}^S h_i x_i - \frac{1}{2} \sum_{i,j=1}^S J_{ij} x_i x_j = 0$. From this equation we obtain the following expression for the probability distribution:

$$P(\mathbf{x}; \mathbf{h}, \mathbf{J}) = e^{- \left(1 + \lambda_0 - \sum_{i=1}^S h_i x_i - \frac{1}{2} \sum_{i,j=1}^S J_{ij} x_i x_j \right)} = \frac{e^{\sum_{i=1}^S h_i x_i + \frac{1}{2} \sum_{i,j=1}^S J_{ij} x_i x_j}}{Z} \tag{6}$$

where Z in the denominator of Eq. (6) is the so-called *partition function* (Pathria and Beale, 2011), which ensures that the distribution is normalized and is given by:

$$Z(\mathbf{h}, \mathbf{J}) = \int \prod_i dx_i e^{\sum_{i=1}^S h_i x_i + \frac{1}{2} \sum_{i,j=1}^S J_{ij} x_i x_j} \equiv e^{1 + \lambda_0}. \tag{7}$$

Eq. (5) can be written in a more compact way in terms of a new vector variable where the vector

$$\mathbf{s} = \mathbf{x} + \mathbf{J}^{-1} \mathbf{h} \text{ as}$$

$$P(\mathbf{s}) = \frac{e^{\frac{1}{2} \sum_{i,j=1}^S J_{ij} s_i s_j}}{Z} = \frac{e^{\frac{1}{2} \mathbf{s}^T \mathbf{J} \mathbf{s}}}{Z}, \tag{6}$$

and Z then becomes

$$Z = \int \prod_i ds_i e^{\frac{1}{2} \sum_{i,j=1}^S J_{ij} s_i s_j} = \int \prod_i ds_i e^{1/2 \mathbf{s}^T \mathbf{J} \mathbf{s}}. \tag{7}$$

Interestingly, the exponent of Eq. (7') is reminiscent of the energy or *hamiltonian* of the widely used spin models in statistical physics (Pathria and Beale, 2011). These *spin* variables, s_i , correspond to microscopic magnetic dipole moments, while J_{ij} are parameters associated to the interaction coefficients between pairs of spins s_i and s_j . If $J_{ij} > 0$ the variables tend to be positively correlated (i.e. the spins tend to be parallel) while if $J_{ij} < 0$ the variables tend to be negatively correlated (i.e. the spins tend to be anti-parallel).

Eq. (7) is a Gaussian integral, which its result is given by an exponential involving the inverse of matrix \mathbf{J} :

$$Z = \frac{(2\pi)^{S/2}}{\sqrt{\det \mathbf{J}}} e^{-1/2 \sum_{i,j=1}^S J_{ij}^{-1} h_i h_j} = \frac{(2\pi)^{S/2}}{\sqrt{\det \mathbf{J}}} e^{-1/2 \mathbf{h}^T \mathbf{J}^{-1} \mathbf{h}}. \tag{8}$$

Now we will show how to relate the unknown vector \mathbf{h} and matrix \mathbf{J} to the known vector \mathbf{m} , with components \bar{x}_i , and the known covariance matrix \mathbf{C} , with components $\bar{x}_i \bar{x}_j - \bar{x}_i \bar{x}_j$. This allows to infer model parameters h_i and J_{ij} from empirical observations such as the means and covariances of the abundances. These relationships can be conveniently obtained from the derivatives of the partition function, which is the standard approach in statistical physics. Indeed, the mean densities can be expressed as

$$m_k \equiv \bar{x}_k = \frac{\int \prod_i dx_i x_k e^{\sum_i h_i x_i + \frac{1}{2} \sum_{i,j=1}^S J_{ij} x_i x_j}}{Z} = \frac{\frac{\partial}{\partial h_k} \int \prod_i dx_i e^{\sum_i h_i x_i + \frac{1}{2} \sum_{i,j=1}^S J_{ij} x_i x_j}}{Z} = \frac{\partial \ln Z}{\partial h_k}. \tag{9a}$$

And, a similar relationship holds for the covariance matrix:

$$C_{ij} \equiv \bar{x}_i \bar{x}_j - \bar{x}_i \bar{x}_j = \frac{\partial^2 \ln Z}{\partial h_i \partial h_j}. \tag{9b}$$

Substituting Eq. (8) into Eq. (9a) and (9b) we get:

$$\mathbf{m} = \mathbf{J}^{-1} \mathbf{h}, \tag{10a}$$

$$\mathbf{C} = -\mathbf{J}^{-1}, \tag{10b}$$

which can be inverted to give:

$$\mathbf{h} = -\mathbf{C}^{-1} \mathbf{m}, \tag{11a}$$

$$\mathbf{J} = -\mathbf{C}^{-1}. \tag{11b}$$

Therefore, using the analogy with the spin models, the matrix \mathbf{J} , which has the natural interpretation of an effective interaction matrix between species, can be obtained as minus the inverse of the covariance matrix. Indeed, the magnitude of J_{ij} corresponds to the strength of the net interaction of species j over species i and that the sign of J_{ij} corresponds to whether this effect is positive or negative (Volkov et al., 2009). Notice that, since the covariance matrix \mathbf{C} has positive elements along the diagonal, the minus sign in the r.h.s. of Eq. (11b) implies that the diagonal elements of \mathbf{J} – corresponding to the intraspecific interaction coefficients – must be negative and thus correspond to intraspecific

competition.

2.2. The covariance matrix exhibits intraspecific elements (variances) much larger than the interspecific ones and this implies the same for the effective interaction matrix

For the eight available censuses – 1982, 1985 and then every five years until 2015 – we observed these two facts about the interspecific elements of the covariance matrix (Fort and Grigera, 2020):

- a) They take both positive and negative values, corresponding respectively to positive and negative correlations (the intraspecific elements $C_{ii} = \overline{(x_i - \bar{x}_i)^2}$, equal to variances σ_i^2 , are by definition always positive).
- b) They are much smaller than the intraspecific ones, by approximately an order of magnitude when taking their absolute values (Table 1).

We will present an heuristic argument, in terms of averages over the S species, denoted by, to show that b) implies that a similar relationship holds for the interspecific interaction coefficients compared with the intraspecific ones. Let us approximate, for each census, the covariance matrix with matrix C^{av} in which all the diagonal elements are equal to $\langle C_{ii} \rangle$ and all off-diagonal elements equal to $\langle C_{ij} \rangle$, where $\langle C_{ii} \rangle$ is the average of the intraspecific covariances (variances), and $\langle C_{ij} \rangle$ the average of the absolute value of the interspecific ones. The absolute value for interspecific elements is taken by a), to avoid cancelations of interspecific covariances with opposite signs when computing averages over species. Therefore, C^{av} can be written as:

$$C^{av} = \langle C_{ii} \rangle \begin{pmatrix} 1 & & & \langle |C_{ij}| \rangle / \langle C_{ii} \rangle \\ & \ddots & & \\ & & \ddots & \\ \langle |C_{ij}| \rangle / \langle C_{ii} \rangle & & & 1 \end{pmatrix} = \langle \sigma_i^2 \rangle \begin{pmatrix} 1 & & & \epsilon \\ & \ddots & & \\ & & \ddots & \\ \epsilon & & & 1 \end{pmatrix}, \tag{12}$$

where $\epsilon \equiv \langle |C_{ij}| \rangle / \langle C_{ii} \rangle$. The inverse of matrix C^{av} can be calculated and produces a simple expression for the effective interaction matrix J^{av} matrix, given by:

$$J^{av} = \frac{1}{\langle \sigma_i^2 \rangle} \frac{1 + (S - 2)\epsilon}{1 + (S - 2)\epsilon - (S - 1)\epsilon^2} \begin{pmatrix} -1 & & & \\ & \ddots & & \\ & & \ddots & \\ & & & \ddots \end{pmatrix} \begin{pmatrix} & & & -\epsilon \\ & & & 1 + (S - 2)\epsilon \\ & & -\epsilon & \\ & 1 + (S - 2)\epsilon & & \ddots \end{pmatrix} \begin{pmatrix} \\ \\ \\ -1 \end{pmatrix} \tag{13}$$

Thus,

Table 1
Mean values of interspecific over intraspecific matrix elements for the eight censuses (dbh > 10 mm). The In the third column the ratios $\langle J_{ij} \rangle / \langle J_{ii} \rangle$ are computed from $J = C^{-1}$; the last column is the formula (15).

census #	$\epsilon \equiv \left \frac{C_{ij}^{av}}{C_{ii}^{av}} \right $	$\langle J_{ij} \rangle / \langle J_{ii} \rangle$	$\epsilon / (1 + 18\epsilon)$
1	0.058	0.054	0.028
2	0.058	0.055	0.028
3	0.054	0.055	0.027
4	0.050	0.046	0.026
5	0.048	0.019	0.026
6	0.046	0.013	0.025
7	0.046	0.015	0.025
8	0.047	0.017	0.026

$$\left| \frac{J_{ij}^{av}}{J_{ii}^{av}} \right| = \frac{\epsilon}{1 + (S - 2)\epsilon} \tag{14}$$

For $S = 20$, we have:

$$\left| \frac{J_{ij}^{av}}{J_{ii}^{av}} \right| \Big/ \left| \frac{J_{ii}^{av}}{J_{ii}^{av}} \right| = \frac{\epsilon}{1 + 18\epsilon}, \tag{15}$$

and ϵ varies between 0.046 and 0.058 across censuses (Table 1), therefore $1 + 18\epsilon$ is always ≈ 2 and thus the ratio $\langle J_{ij} \rangle / \langle J_{ii} \rangle$ computed from $J = C^{-1}$, is always (smaller but) comparable to $\epsilon \equiv \left| \frac{C_{ij}^{av}}{C_{ii}^{av}} \right|$.

Hence, on average, the empirically observation that the variances of the species abundances are much larger than the covariances between the abundances of different species implies that the intraspecific effective interaction coefficients are much larger than the interspecific ones.

2.3. The intraspecific competition coefficients play a central role in controlling the dynamics of species

The above conclusion that $|C_{ij}| / |C_{ii}| \ll 1$ implies that $|J_{ij}| / |J_{ii}| \ll 1$, together with the result that keeping only intraspecific competition is enough to predict the overall evolution of the abundances of tree species with remarkable accuracy (Fort and Grigera, 2020), lead us to focus on analyzing the dynamics of the intraspecific interaction coefficients along censuses to anticipate drastic changes in species abundances. Thus, we compare $J_{ii}(c)$, where c denotes the census number, against abundance trajectories $N_i(c) = \bar{x}_i(c)A$ (where $A = 50,000 \text{ m}^2$ is the total area of the plot).

3. Results

The abundance trajectories $N_i(c)$ for these 20 most abundant species varied from monotonic growth to oscillations and busts (Fig. 1a).

Let us focus on those species that have experienced severe population crashes, i.e. decreases of their abundance greater than 50% respect to the first census in 1982. They comprise three species: *Psychotria horizontalis*, *Piper cordulatum* and *Poulsenia armata* (see Fig. 1a). *Piper cordulatum* is the species that experienced the most drastic bust; after an initial population growth from 1982 to 1985 its abundance crashed by almost 100% for the 5th census in 2000.

Fig. 1b shows the variation of the species abundances vs. the intraspecific interaction coefficient $J_{ii}(c)$ for the eight censuses. Notice that in general they parallel the evolution of the corresponding abundance trajectory $N_i(c)$ for $i = 1, 2, \dots, 20$. In particular the three crashing species also exhibit drastic drops of their effective intraspecific competition coefficients $J_{ii}(c)$.

For these three species, in order to make a standardized comparison between the drops of $N_i(c)$ and $J_{ii}(c)$, we computed the percentage variation along censuses 2 to 8 with respect to census 1 of the two quantities. Fig. 2 shows that the drop of $J_{ii}(c)$ is steeper than the corresponding one for the $N_i(c)$. We show results both for $\text{dbh} \geq 25 \text{ mm}$ (Fig. 2a), and $\text{dbh} \geq 10 \text{ mm}$ (Fig. 2b). Notice that for all the three species the earliness of a 50% or larger decrease of $J_{ii}(c)$ with respect to the one for $N_i(c)$ is bigger for $\text{dbh} \geq 10 \text{ mm}$ than for $\text{dbh} \geq 25 \text{ mm}$. This earliness increases from 5 years ($\text{dbh} \geq 25 \text{ mm}$) to 15 years ($\text{dbh} \geq 10 \text{ mm}$) for *Psychotria horizontalis*; from 0 to 5 years for *Piper cordulatum* and from 5 to 10 years for *Poulsenia armata*.

As we have shown in the previous section, the fact that the intraspecific elements of J_{ij} are much larger than the interspecific elements is linked with the fact that the same happens for the covariance matrix. Fig. 3 compares for the three crashing species the evolution of $J_{ii}(c)$ and of $\sigma_i^2(c)$. Notice that the drop of $J_{ii}(c)$ is steeper than the corresponding one for $\sigma_i^2(c)$.

Table 2 shows the percentage difference of $1/\sigma_i^2$ relative to J_{ii} for the 20 most abundant species across the eight censuses.

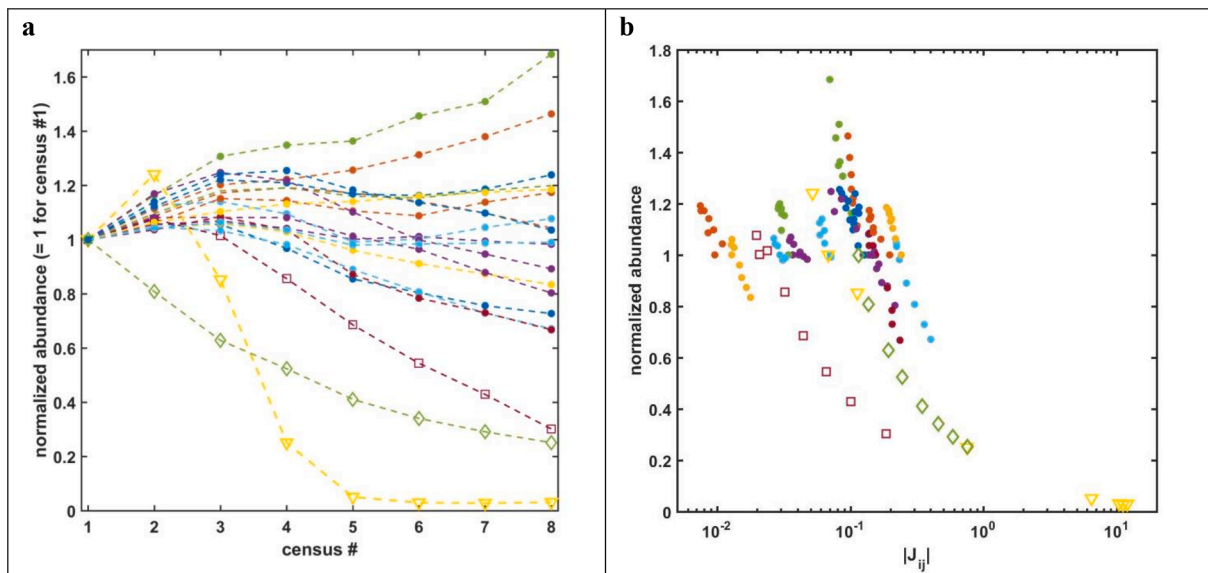


Fig. 1. Variation of the abundances of the 20 most abundant species and of their corresponding intraspecific competition coefficients for dbh ≥ 10 mm along the eight censuses. The abundances are normalized by dividing with respect to the value at the first census (1982). Species # 7 *Psychotria horizontalis* (diamonds), species # 10 *Piper cordulatum* (triangles) and *Poulsenia armata* species # 19 (squares). **a.** Normalized abundances vs. census number. **b.** Normalized abundances vs. absolute value of the intraspecific competition coefficient (log scale) along different censuses.

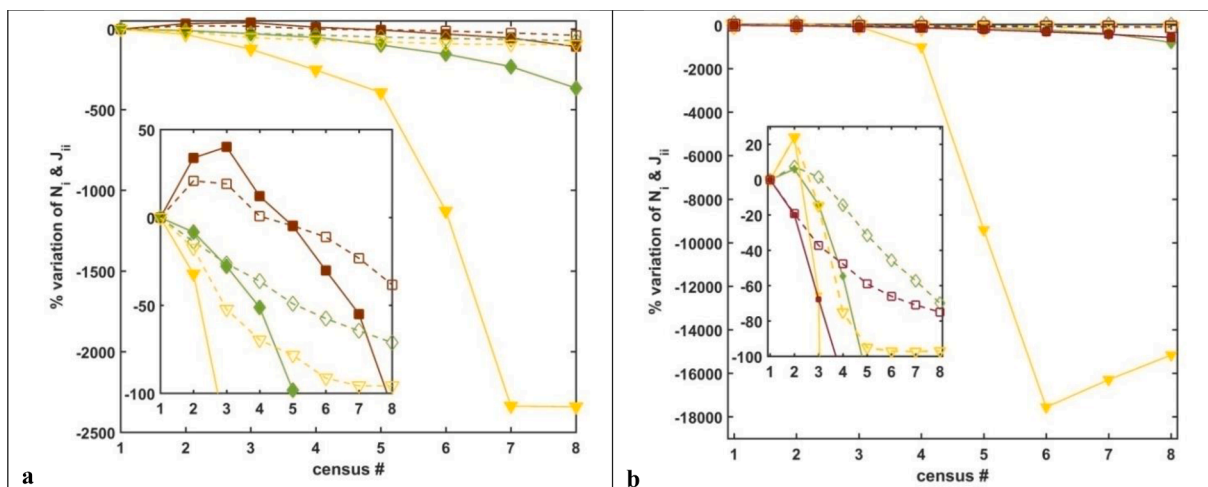


Fig. 2. Percentage variations of the abundances (dashed lines) and intraspecific competition coefficients (filled lines) for the three species that experienced steep declines along the eight censuses, respect to the first census (1982). **a:** dbh ≥ 25 mm **b:** dbh ≥ 10 mm. Species # 7 *Psychotria horizontalis* (diamonds), species # 10 *Piper cordulatum* (triangles) and *Poulsenia armata* species # 19 (squares). The insets are zoom-in plots to allow comparisons of the drops in both variables for each species.

Finally, we were interested in checking the well known empirical Taylor’s law (Taylor, 1961), i.e. that the variance of species population density scales as a power-law function of the mean population density for the set of selected 20 species.

We found that all the 20 species verify that the variance for census # c scales with the population density for this census as

$$\sigma_i^2(c) = a_i \bar{x}_i(c)^{b_i}, \tag{16}$$

where $a_i > 0$ and the exponents b_i , obtained by linear regression, are listed in the last column of Table 2.

4. Discussion

The MaxEnt principle can be viewed as an inference method in which we have to select some set of empirical observations as constraints. In

this study we took the spatial covariance matrix of species’ abundances in quadrats. The rationale for this was that pairwise species interactions are enough to capture the behavior of a tree community. In order to take this description seriously, the goodness of this choice must be tested. Indeed, it could be that the tangle of complex biotic and abiotic interactions cannot be correctly described by pairwise maximum entropy modeling. We have previously shown (Fort and Grigera, 2020; Fort, 2020) that these models provide a reasonable description of the BCI tree community. Furthermore, in a first approximation, the effect of the interspecific interactions can be neglected compared to the intraspecific ones.

As shown in Figs. 1 and 2, the effective intraspecific interaction coefficient J_{ii} , estimated via MaxEnt, provides a clear early warning indicator of impending population crashes for species of trees. There are three species that experimented population crashes (reductions of more than 50% in the number of individuals) along the last 35 years:

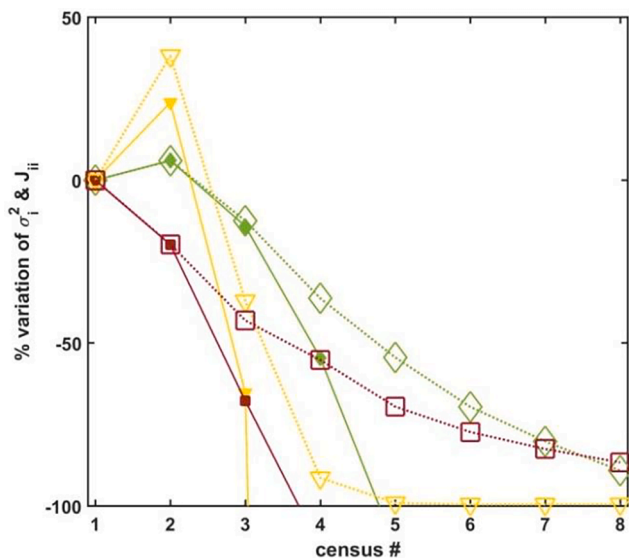


Fig. 3. Percentage variations of the variances (dotted lines) and intraspecific competition coefficients (filled lines) for the three species that experienced steep declines along the eight censuses (dbh ≥ 10 mm), respect to the first census (1982). Species # 7 *Psychotria horizontalis* (diamonds), species # 10 *Piper cordulatum* (triangles) and *Poulsonia armata* species # 19 (squares).

Psychotria horizontalis, *Piper cordulatum* and *Poulsonia armata*. They all exhibit a steeper earlier drop of $J_{ii}(c)$ than their abundances $N_i(c)$ (at least five years before). This can be easily explained from the empirical fact that the exponents of the Taylor’s power law for these three species are larger than 1 (see the last column of Table 2). As we have seen, due to the also empirical fact that the interspecific interactions in BCI are negligible respect to the intraspecific ones, the intraspecific effective competition coefficients can be approximated by the inverse of the variances (see Eq. (13)). And, combining this with the Taylor’s power law Eq. (16) we can approximate the intraspecific interaction coefficients as:

$$J_{ii}(c) \approx \frac{1}{\sigma_i^2(c)} = \frac{1}{a_i \bar{x}_i(c)^{-b_i}} \tag{17}$$

Table 2
Percentage of difference of $1/\sigma_i^2$ relative to J_{ii} and Taylor’s exponent in Eq. (16) for the 20 most abundant species (dbh > 10 mm). Highlighted in bold are those species which experimented population crashes.

species name	Census (year)								Exponent <i>b</i>
	1982	1985	1990	1995	2000	2005	2010	2015	
<i>Hybanthus prunifolius</i>	21	19	14	13	11	13	12	12	1.21
<i>Faramea occidentalis</i>	39	37	38	36	31	30	29	30	1.69
<i>Trichilia tuberculata</i>	22	23	23	23	24	24	27	24	1.29
<i>Desmopsis panamensis</i>	11	11	11	10	10	11	9	10	3.07
<i>Alseis blackiana</i>	15	15	13	12	11	10	9	9	0.52
<i>Mouriri myrtilloides</i>	34	36	33	30	25	24	25	30	1.72
<i>Psychotria horizontalis</i>	18	17	18	16	14	13	12	13	1.78
<i>Hirtella triandra</i>	31	28	26	24	22	23	24	24	1.81
<i>Garcinia intermedia</i>	11	11	12	10	9	10	11	11	0.66
<i>Piper cordulatum</i>	16	22	21	11	5	4	5	5	1.46
<i>Capparis frondosa</i>	20	20	18	15	14	12	13	13	1.69
<i>Tetragastris panamensis</i>	27	26	27	26	24	23	22	22	1.04
<i>Sorocea affinis</i>	15	15	14	14	13	14	16	14	1.33
<i>Tachigali versicolor</i>	19	19	21	18	15	12	6	7	1.37
<i>Protium tenuifolium</i>	34	37	35	34	35	39	42	44	1.27
<i>Protium panamense</i>	36	37	35	31	29	24	21	23	1.79
<i>Swartzia simplex</i>	15	15	16	15	14	15	15	15	1.39
<i>Beilschmiedia pendula</i>	28	22	23	24	24	25	23	22	2.72
<i>Poulsonia armata</i>	46	40	39	39	34	33	32	29	1.47
<i>Rinorea sylvatica</i>	5	5	4	4	4	4	4	4	2.28
mean	23	23	22	20	19	18	18	18	

From expression (17) it is easy to show that

$$\frac{dJ_{ii}(c)}{J_{ii}(c)} \approx -b_i \frac{d\bar{x}_i(c)}{\bar{x}_i(c)}, \tag{18}$$

and thus, since $b_i > 1$ for these three species (in fact $b_i > 1$ for 18 out of the 20 considered species), the relative changes of the intraspecific effective competition coefficients are larger than the relative changes experimented by the population densities. This result, besides providing additional support to the rightness of the MaxEnt description, it offers an observable to monitor to anticipate population busts.

From Fig. 2, it is seen that the early warning signal is stronger when using the full census (dbh > 10 mm, Fig. 2b) than when using only dbh > 25 mm (Fig. 2a). This corresponds to steeper abundance drops for the full census, and is probably connected that with the lower dbh threshold, more saplings are included in the population. Indeed, it has been found that population changes were most pronounced in saplings, and in particular, saplings of the species considered in Fig. 2 showed conspicuously higher mortality (Condit et al., 2017).

Looking at Eq. (6) one may wonder whether the other set of parameters appearing in the probability distribution $P(x; \mathbf{h}, \mathbf{J})$, i.e. \mathbf{h} , also provide an early warning signal for crashing species. Indeed it does. This is because, from Eqs. (9a), (11a) and (11b) we get $h_i(c) = \sum_{j=1}^S J_{ij}(c) \bar{x}_j(c) = \sum_{j=1}^S J_{ij}(c) N_j(c) / A$. Therefore, as an early warning signal, it interpolates between $N_i(c)$ and $J_{ii}(c)$: it is better that the first but worse than the second.

It is worth noticing that the factor $\frac{1+(S-2)\epsilon}{1+(S-2)\epsilon-(S-1)\epsilon^2}$ appearing in Eq. (13) for ϵ varying empirically among censuses between 0.046 and 0.058, is always ≈ 1 . Therefore, the average (over species) intraspecific effective competition coefficient $\langle J_{ii} \rangle$ is well approximated by $1/\sigma_i^2$. An interesting question is for each species i how close is J_{ii} to $1/\sigma_i^2$. Table 2 shows that the percentage difference varies from the 20 species across the eight censuses between 4 and 46 % (mean of 20%). Hence, the early warning signal we are proposing is connected with the jump of the corresponding species variance (Fig. 3). This can be easily understood since the diagonal coefficients of matrix \mathbf{C} , the variances σ_i^2 , are much greater than the off-diagonal covariances explaining therefore their disproportionate contribution to the intraspecific interaction coefficients. This is an interesting result since an anomalous (large) variance is known to be a red flag anticipating an upcoming population drop (Fernández and Fort, 2009; Donangelo et al., 2010; Dakos et al., 2010).

That is, the variances may be used as early warnings in communities of coexisting species in cases in which covariances are not known. However, J_{ii} , which comes from the inverse of the covariance matrix, thus includes information from the whole community *i.e.* more information than σ_i^2 . And, as shown by Fig. 3, $J_{ii}(c)$ provides an earlier warning signal than $\sigma_i^2(c)$ of ongoing species population crashes.

Changes in environmental conditions can trigger a sudden collapse of ecological communities (Scheffer et al., 2001; Boettiger et al., 2013), with serious consequences for human well-being (Millennium Ecosystem Assessment, 2005). There are empirical evidences that diversity loss increases vulnerability to ecosystem collapse (MacDougall et al., 2013). This is why devising indicators that work as early warnings of severe decreases in the abundance of species, generated from empirical data, is an important task.

5. Conclusion

In summary, we found that:

- I) For each species i the absolute value of the intraspecific competition coefficients for all census c , $J_{ii}(c) < 0$, is much larger than those of the interspecific interaction coefficients $J_{ij}(c)$ with $i \neq j$ (which are of both signs).
- II) The above result, $|J_{ii}| \gg |J_{ij}|$, can be derived from a similar empirical relationship observed for the covariance matrices, *i.e.* $|C_{ij}| \ll C_{ii} \equiv \sigma_i^2$.
- III) For those tree species that crashed or suffered steep population declines across the eight tree censuses the drop of J_{ii} is always steeper than the drop of the corresponding abundance N_i .
- IV) Using the full population data ($\text{dbh} \geq 10$ mm) improves the quality of the early warning signal respect when using just a subset of larger trees ($\text{dbh} \geq 25$ mm). This is probably connected with the conspicuously higher mortality of saplings found for species that crashed (Condit et al., 2017).
- V) Indeed, for $\text{dbh} \geq 10$ mm, 50%+ decreases in J_{ii} occur between 5 and 15 years in advance than comparable declines for the abundances N_i .
- VI) By II), the drop of J_{ii} is linked to the anomalous variance, which is a known early warning of incoming catastrophic shifts. However, the sudden increase in the intraspecific competition, besides being more illuminating from a conceptual population dynamics modeling perspective, it provides a sharper signal than the jump in σ_i^2 .

Therefore we conclude that the monitoring the intraspecific effective interaction terms J_{ii} for tree species across censuses serves as an early warning indicator of an impending population bust; steep declines in J_{ii} always occur several years in advance of comparable population drops.

Declaration of Competing Interest

The authors declare that they have no known competing financial interests or personal relationships that could have appeared to influence the work reported in this paper.

Acknowledgements

The authors thank support from project ERANET-LAC R&I2016-1005422.

We acknowledge the support of the Center for Tropical Forest Science for providing data for the BCI plot (Condit 2019). T. G. thanks Universidad de la República (Montevideo) for hospitality.

We are grateful with two anonymous referees; their criticism on a previous version of the manuscript served to greatly improve the clarity of presentation of our work.

References

- Adler, P.B., et al., 2018. Competition and coexistence in plant communities: intraspecific competition is stronger than interspecific competition. *Ecol. Lett.* 21, 1319–1329.
- Adler, P.B., HilleRisLambers, J., Levine, J.M., 2007. A niche for neutrality. *Ecol. Lett.* 10, 95–104.
- Arfken, G., 1985. Lagrange Multipliers. In: §17.6 in *Mathematical Methods for Physicists*, 3rd ed. Academic Press, Orlando, FL, pp. 945–950.
- Boettiger, C., Ross, N., Hastings, A., 2013. Early warning signals: the charted and uncharted territories. *Theor. Ecol.* 6, 255–264.
- Brummer, A., Newman, E., 2019. Derivations of the core functions of the maximum entropy theory of ecology. *Entropy* 21, 712.
- Carpenter, S.R., et al., 2011. Early Warnings of Regime Shifts: A Whole-Ecosystem Experiment. *Science* 332, 1079–1082.
- Chase, J.M., 2014. Spatial scale resolves the niche versus neutral theory debate. *J. Veg. Sci.* 25, 319–322.
- Chesson, P., 2000. Mechanisms of maintenance of species diversity. *Annu. Rev. Ecol. Syst.* 31, 343–366.
- Clark, J.S., McLachlan, J.S., 2003. Stability of forest biodiversity. *Nature* 423, 635–638.
- Condit, R., et al., 2017. Demographic trends and climate over 35 years in the Barro Colorado 50 ha plot. *Forest Ecosystems* 4, art numb.17.
- Dakos, V.N., Nes, E.H., Donangelo, R., Fort, H., Scheffer, M., 2010. Spatial correlation as leading indicator of catastrophic shifts. *Theor. Ecol.* 3, 163–174.
- Doncaster, C.P., et al., 2016. Early warning of critical transitions in biodiversity from compositional disorder. *Ecology* 97, 3079–3090.
- Donangelo, R., Fort, H., Dakos, V., Scheffer, M., van Nes, E.H., 2010. Early warnings for catastrophic shifts in ecosystems: comparison between spatial and temporal indicators. *Int. J. Bifurcation Chaos* 20, 315–321.
- Fernández, A., Fort, H., 2009. Catastrophic phase transitions and early warnings in a spatial ecological model. *J. Stat. Mech. Theory Exp.* 09, P09014.
- Fort, H., Segura, A., 2018. Competition across diverse taxa: quantitative integration of theory and empirical research using global indices of competition. *Oikos* 127, 392–402.
- Fort, H., Grigera, T., 2020. A method for predicting changes in species abundances makes accurate forecasts for trees in tropical forests. Submitted to. *Ecol. Model.*
- Fort, H., 2020. Ecological Modelling and Ecophysics: Agricultural and environmental applications (IOP ebooks), IOP, Bristol, UK.
- Garzon-Lopez, C.X., Jansen, P.A., Bohlman, S.A., Ordóñez, A., Olff, H., 2014. Effects of sampling scale on patterns of habitat association in tropical trees. *J. Veg. Sci.* 25, 349–362.
- Hooper, D.U., et al., 2012. A global synthesis reveals biodiversity loss as a major driver of ecosystem change. *Nature* 486, 105–108.
- Hubbell, S.P., 2008. Approaching tropical forest complexity, and ecological complexity in general, from the perspective of symmetric neutral theory. In: Carson, W., Schnitzer, S. (Eds.), *Tropical Forest Community Ecology*. Wiley-Blackwell, New York.
- Hubbell, S.P., 2009. Neutral theory and the theory of island biogeography. In: Losos, J., Ricklefs, R.E. (Eds.), *The Theory of Island Biogeography at 40: Impacts and Prospects*. Princeton University Press, Princeton, NJ.
- Ishida, A., et al., 2003. Leaf physiological adjustments to changing lights: partitioning the heterogeneous resources across tree species. *Pasoh: Ecology of a lowland rain forest in Southeast Asia*. Springer.
- Ives, A.R., Carpenter, S.R., 2007. Stability and diversity of ecosystems. *Science* 317, 58–62.
- Jaynes, E.T., 1957a. Information theory and statistical mechanics I. *Phys. Rev.* 106, 620–630.
- Jaynes, E.T., 1957b. Information theory and statistical mechanics II. *Phys. Rev.* 108, 171–190.
- Jaynes, E.T., 1982. On the rationale of maximum entropy methods. *Proc. Instit. Elec. Electron. Eng.* 70, 939–952.
- MacDougall, A.S., McCann, K.S., Gellner, G., Turkington, R., 2013. Diversity loss with persistent human disturbance increases vulnerability to ecosystem collapse. *Nature* 494, 86–90.
- Millennium Ecosystem Assessment, 2005. *Ecosystems and Human Well-being: Synthesis Report*, Island.
- Pathria, R.K., Beale, P.D., 2011. *Statistical Mechanics*, third ed., Butterworth Heinemann.
- Saravia, L.A., Momo, F.R., 2018. Biodiversity collapse and early warning indicators in a spatial phase transition between neutral and niche communities. *Oikos* 127, 111–124.
- Scheffer, M., Carpenter, S.R., 2003. Catastrophic regime shifts in ecosystems: linking theory to observation. *Trends Ecol. Evol.* 12, 648–656.
- Scheffer, M., et al., 2001. Catastrophic shifts in ecosystems. *Nature* 413, 591–596.
- Shannon, C., 1948. A mathematical theory of communication. *Bell Syst. Tech. Jour.* 27, 379–423.
- Suweis, S., D'Odorico, P., 2014. Early Warning Signs in Social-Ecological Networks. *PLoS ONE* 9, e101851.
- Taylor, L.R., 1961. Aggregation, variance and the mean. *Nature* 189, 732–735.
- Thompson, R., Starzomski, B.M., 2006. What does biodiversity actually do? A review for managers and policy makers. *Biodivers. Conserv.* 16, 1359–1378.
- Volkov, I., Banavar, J.R., Hubbell, S.P., Maritan, A., 2009. Inferring species interactions in tropical forests. *PNAS* 106, 13854–13859.
- Whittaker, R.H., 1975. *Communities and Ecosystems*. MacMillan, New York.